The Plant Cell, Vol. 21: 1182–1194, April 2009, www.plantcell.org © 2009 American Society of Plant Biologists

Suppression of Repeat-Mediated Gross Mitochondrial Genome Rearrangements by RecA in the Moss *Physcomitrella patens* [C][W]

Masaki Odahara, Haruko Kuroiwa, Tsuneyoshi Kuroiwa, and Yasuhiko Sekine[1]

Department of Life Science, College of Science, Rikkyo (St. Paul's) University, Toshima-ku, Tokyo 171-8501, Japan

RecA and its ubiquitous homologs are crucial components in homologous recombination. Besides their eukaryotic nuclear counterparts, plants characteristically possess several bacterial-type RecA proteins localized to chloroplasts and/or mitochondria, but their roles are poorly understood. Here, we analyzed the role of the only mitochondrial RecA in the moss *Physcomitrella patens*. Disruption of the *P. patens* mitochondrial *recA* gene *RECA1* caused serious defects in plant growth and development and abnormal mitochondrial morphology. Analyses of mitochondrial DNA in disruptants revealed that frequent DNA rearrangements occurred at multiple loci. Structural analysis suggests that the rearrangements, which in some cases were associated with partial deletions and amplifications of mitochondrial DNA, were due to aberrant recombination between short (<100 bp) direct and inverted repeats in which the sequences were not always identical. Such repeats are abundant in the mitochondrial genome, and interestingly many are located in group II introns. These results suggest that RECA1 does not promote but rather suppresses recombination among short repeats scattered throughout the mitochondrial genome, thereby maintaining mitochondrial genome stability. We propose that RecA-mediated homologous recombination plays a crucial role in suppression of short repeat-mediated genome rearrangements in plant mitochondria.

INTRODUCTION

Plant mitochondria play a vital role in the cell as the major producers of ATP via oxidative phosphorylation, and they provide metabolic intermediates that serve as substrates for the synthesis of nucleic acids, amino acids, and fatty acids. Plant mitochondrial genomes encode only a small number of RNAs and proteins, including rRNAs, tRNAs, some subunits of respiratory chain complexes, and a few ribosomal proteins (Oda et al., 1992; Unseld et al., 1997). Most of the reported mutations in mitochondrial genes affect plant growth and development (Newton et al., 2004). Characteristically, the rate of nucleotide substitutions in plant mitochondrial genomes is generally lower than that in plant nuclear and chloroplast genomes (Wolfe et al., 1987; Palmer and Herbon, 1988). Most of the reported mitochondrial mutations are rearrangements and deletions caused by aberrant recombination between short (generally <200 bp) repeats (Newton et al., 2004). These recombination events are the main source of mitochondrial mutations that confer cytoplasmic male sterility and nonchromosomal stripe, a maternally inherited mutation that confers variable leaf striping and poor growth (Newton et al., 2004), and they are also thought to contribute to the relatively rapid structural evolution of mitochondrial genomes (Small et al., 1989). In addition to the short repeats, which commonly exist in lower and higher plant mitochondrial genomes (Andre et al., 1992), higher plant mitochondrial genomes uniquely contain at least one pair of long repeats (>1 kb), which when oriented as direct repeats may be involved in frequent homologous recombination to generate subgenomic molecules (Lonsdale et al., 1984). Thus, recombination is deeply involved in the dynamics of plant mitochondrial genomes, although the mechanisms underlying these dynamics are still largely unknown.

RecA is a crucial component in homologous recombination and recombinational DNA repair in bacteria. RecA binds to DNA to form a nucleoprotein filament, which then aligns with a homologous DNA duplex to promote single-strand exchange (Lusetti and Cox, 2002). Mutation of *recA* confers a dramatic reduction not only in the efficiency of homologous recombination but also in the extent of cellular tolerance to DNA damage. This is because RecA has multiple functions in SOS induction (Little and Mount, 1982) and mutagenic lesion bypass synthesis during the SOS response (Pham et al., 2001), besides its direct role in recombinational repair. Recent studies suggest a significant role for RecA and other recombination proteins in the repair of stalled or collapsed replication forks (Cox et al., 2000; Lusetti and Cox, 2002).

Homologs of RecA have been identified in many prokaryotes and eukaryotes. The higher plant *Arabidopsis thaliana* features Rad51 and Dmc1, eukaryotic counterparts for nuclear DNA recombination/repair (Bishop et al., 1992; Shinohara et al., 1992), and several bacterial-type RecA homologs encoded in the nucleus, which have been shown to be targeted to chloroplasts (Cerutti et al., 1992; Cao et al., 1997) and/or mitochondria

[1] Address correspondence to ysekine@rikkyo.ac.jp.
The author responsible for distribution of materials integral to the findings presented in this article in accordance with the policy described in the Instructions for Authors (www.plantcell.org) is: Yasuhiko Sekine (ysekine@rikkyo.ac.jp).
[C]Some figures in this article are displayed in color online but in black and white in the print edition.
[W]Online version contains Web-only data.
www.plantcell.org/cgi/doi/10.1105/tpc.108.064709

(Khazi et al., 2003; Shedge et al., 2007). RecA-like strand transfer activity has been detected in a stromal extract from pea (*Pisum sativum*) chloroplasts (Cerutti and Jagendorf, 1993) and in soybean (*Glycine max*) mitochondria (Manchekar et al., 2006). In the moss *Physcomitrella patens*, two RecA homologs were identified, a mitochondrial-targeted RecA (RECA1) and a chloroplast-targeted RecA (RECA2) (Odahara et al., 2007; Inouye et al., 2008). The *RECA1* gene disruptant exhibits a lower rate of recovery of the mitochondrial DNA (mtDNA) from methyl methanesulfonate (MMS)-induced damage (Odahara et al., 2007), suggesting the involvement of *RECA1* in the repair of mtDNA.

The nuclear genome of *P. patens*, in which gene targeting occurs with an efficiency similar to that observed in yeast (Schaefer, 2001), was recently sequenced (Rensing et al., 2008), and the chloroplast and the mitochondrial genomes were previously sequenced (Sugiura et al., 2003; Terasawa et al., 2007), enabling advanced genetic and molecular biological approaches to be used in this organism. Here, we analyzed the in vivo roles of the *P. patens* mitochondrial RecA protein RECA1 by targeted nuclear gene inactivation. Disruption of the *RECA1* gene resulted in a remarkable defect in plant growth and gross rearrangements of the mitochondrial genome. Our structural analysis of the rearranged DNA showed that recombination among short dispersed repeats was induced in the disruptants. Based on our results, we discuss an important role of bacterial-type RecA in maintaining mitochondrial genome stability and the possible implications of our findings for the evolution of the plant mitochondrial genome.

RESULTS

Disruption of *RECA1* Causes Serious Defects in Growth and Development of *P. patens*

To investigate the role of RECA1 in planta, we generated *RECA1* gene disruptants by homologous recombination using a targeting construct in which a neomycin phosphotransferase gene (*nptII*) cassette was inserted into the middle of the genomic *RECA1* sequence (Figure 1A). Two of three independently obtained *RECA1* disruptants [*recA1(ins)-1* and *-2*] were selected for further analysis, as they showed very similar phenotypes. In these disruptants, proper integration of one copy of the *nptII* cassette into the genomic *RECA1* locus and the absence of a *RECA1* transcript originating downstream of the inserted *nptII* cassette were confirmed by DNA gel blot analysis (Figure 1B) and RT-PCR analysis (Figure 1C), respectively.

In the early stage of the formation of a *P. patens* colony starting from a small cluster of cells on an agar medium, filamentous cells called protonemata grow to make a network of filaments. Subsequently, gametophores resembling a small plant with leaves and root-like rhizoids develop from a fraction of the protonemata. To investigate the influence of *RECA1* gene disruption on *P. patens* cell growth and development, *RECA1* disruptant colonies formed on agar medium were compared with wild-type colonies. *RECA1* disruptants exhibited obvious defects in growth rate; their surface area was significantly reduced compared with that of wild-type colonies (Figures 1D and 1F). Besides the reduction in growth rate, gametophores barely developed in *RECA1* disruptant colonies cultivated for 4 weeks (Figure 1D). The protonemata of *RECA1* disruptants were shorter than those of wild-type colonies, and in particular, the lengths of the apical cells were significantly reduced (Figure 1E). The protonemata of the *RECA1* disruptant appeared darker than did those of wild-type plants because the chloroplast density was higher in *RECA1* disruptant cells, which had a reduced volume compared with wild-type cells (Figure 1E). Judging from these cell morphologies, the elongation of disruptant cells appeared to be inhibited.

Abnormal Mitochondria in *RECA1* Disruptant Cells

The RECA1 protein has been shown to be targeted to mitochondria (Odahara et al., 2007), strongly suggesting that this organelle is primarily affected by disruption of the *RECA1* gene. Ultrastructural analysis of protonema by transmission electron microscopy revealed obvious abnormalities of mitochondrial structure in the *RECA1* disruptant as follows. Whereas wild-type mitochondria contained developed cristae that resembled small rings (Figures 2A and 2C), by contrast, disruptant mitochondria were enlarged and contained vacuolated cristae (Figures 2B, 2D, and2 E). The disruptant mitochondrial matrix stained less intensely than did the wild-type matrix (Figures 2C to 2E), suggesting a lower electron density of the mitochondrial matrix. In addition, abnormally extended mitochondria were often observed in *RECA1* disruptants (Figure 2F). The apparent abnormalities in the structure of the disruptant mitochondria revealed by transmission electron microscopy suggest that *RECA1* disruptant mitochondria are dysfunctional. It should be added that the *RECA1* disruption also affected the ultrastructure of chloroplasts, which were abnormally shaped and had reduced amounts of thylakoid membrane (Figure 2B). However, the defects of chloroplasts would not be a special case, as it is well established that photosynthetic function can be reduced in the mitochondrial electron transport mutant (Gu et al., 1993; Jiao et al., 2005).

Specific Rearrangements of *RECA1* Disruptant Mitochondrial DNA

Escherichia coli RecA contributes to the maintenance of genomic DNA via recombinational DNA repair. Because RECA1 was suggested to participate in the repair of mtDNA, like *E. coli* RecA (Odahara et al., 2007), we examined the effect of the *RECA1* disruption on mtDNA copy number. To estimate the copy number of mtDNA relative to that of nuclear DNA, we performed DNA gel blot analysis. The intensity of a 3.3-kb *Eco*RI fragment derived from the mitochondrial *nad2* locus was divided by that of a 10.5-kb *Eco*RI fragment derived from the nuclear *GAPDH* locus (Figure 3A). There was no significant difference in the relative mtDNA copy number between wild-type and the two *RECA1* disruptant strains (Figure 3A), indicating that the *RECA1* disruptants bear a normal copy number of mtDNA at the *nad2* locus. However, we observed two additional subsignals, a 2.2-kb *Eco*RI fragment seen in both the wild-type and the *RECA1* disruptants and a 1.8-kb *Eco*RI fragment seen only in the disruptants (Figure 3A). Since the two *RECA1* disruptants were independently obtained, the presence of this latter fragment suggests that a specific DNA rearrangement occurred in the disruptant mtDNA.

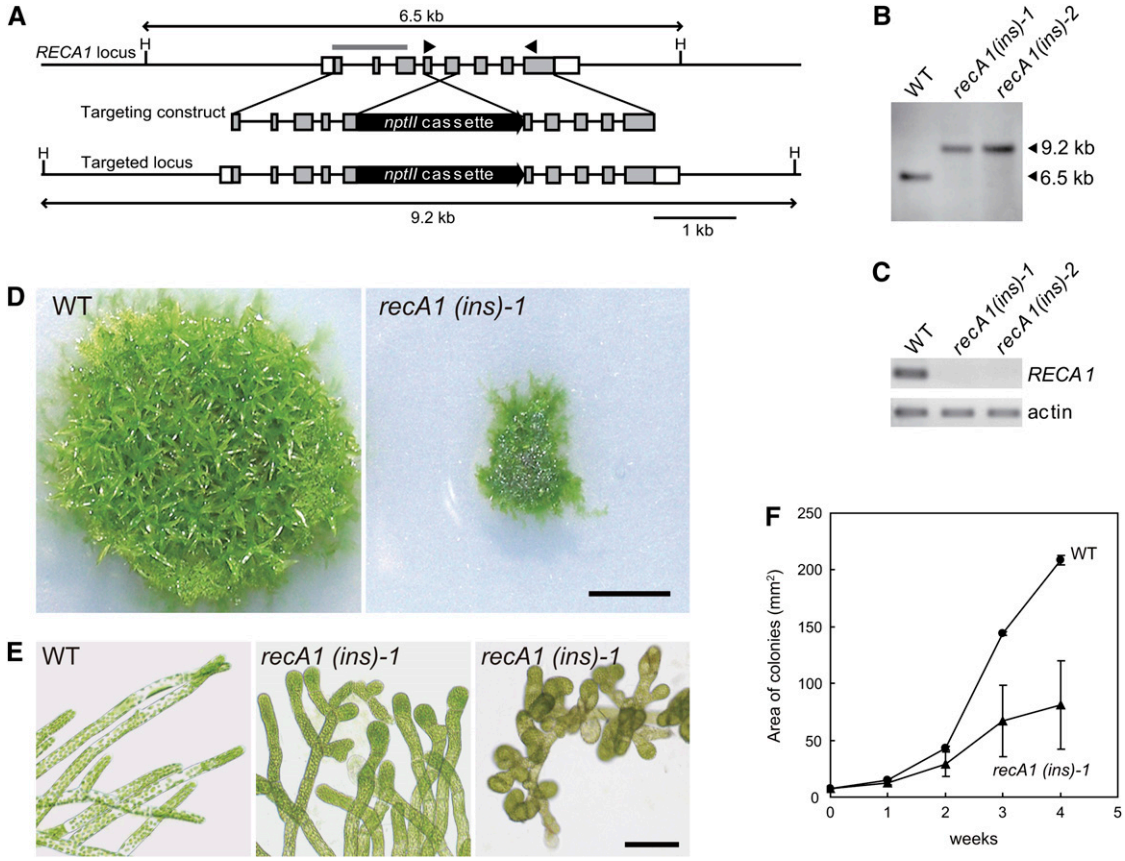

Figure 1. Generation of *RECA1* Insertional Disruptants and Their Growth and Development.

(A) Scheme for the disruption of the *RECA1* locus. The boxes represent exons, and the lines between boxes represent introns and noncoding flanking sequences of *RECA1*. The coding regions are shaded in gray. The *Hin*dIII recognition sites are indicated by H. The location of the probe and the primers used in **(B)** and **(C)** are shown by a bold gray line and arrowheads, respectively. The *nptII* cassette consists of the cauliflower mosaic virus 35S promoter-driven neomycin phosphotransferase II gene.

(B) DNA gel blot analysis of the *RECA1* locus in two *RECA1* insertional disruptants [*recA1(ins)-1* and *recA1(ins)-2*]. Total genomic DNA was digested with *Hin*dIII and hybridized to the *RECA1* probe. The lengths of the bands are indicated on the right.

(C) RT-PCR analysis of the *RECA1* transcript in *RECA1* disruptants.The PCR was repeated twice with similar results.

(D) and **(E)** Morphology of colonies **(D)** and protonemata **(E)** in the wild-type background and of the *RECA1* disruptant cultivated on agar medium for 4 weeks. Bars = 5 mm in **(D)** and 100 μm in **(E)**.

(F) Growth rates of wild-type and *RECA1* disruptant colonies. Data are expressed as mean ± SD (n = 3).

To characterize this rearrangement, we analyzed the structures of the all three *Eco*RI fragments (3.3, 2.2. and 1.8 kb) that hybridized to the *nad2* probe. Cloning and sequencing of the *nad2*-related DNA fragments indicated the following: the 3.3-kb fragment was a segment of the mitochondrial *nad2* locus to which the *nad2* probe was originally designed to hybridize, and the 2.2-kb fragment was a segment of the mitochondrial *atp9* locus with a 69-bp sequence that is highly similar (91% identity) to a sequence in the *nad2* locus, which explains why this fragment was detected using the *nad2* probe. A clone of the *RECA1* disruptant-specific 1.8-kb fragment (named N18-1) was a segment of a sequence essentially identical to the *nad2* sequence except for a 69-bp sequence, in which the sequence identity was switched from *nad2* to *atp9* (Figures 3B and 3C). This shows that the 1.8-kb fragment was derived from recombination involving the *nad2* and *atp9* loci. Similar analysis of two other clones of the 1.8-kb fragments (N18-2 and -3) revealed that they were segments of a *nad2-atp9* recombinant in which the recombination junction also resides within the 69-bp sequence but which was different from that of the clone N18-1 (Figure 3C). These results indicate an accumulation of DNA molecules derived from aberrant recombination between the 69-bp sequences present in both the *nad2* and *atp9* loci in *RECA1* disruptant mitochondria.

Suppression of *RECA1* Disruptant Phenotypes by Overexpression of *RECA1* cDNA

In the *RECA1* disruptant, which was constructed by insertion of the *nptII* cassette into the middle of the coding region, a truncated form of the RECA1 protein could be produced from the remaining 5′ half of the coding region (Figure 1A). The recombination between short repeats in the disruptant mitochondria

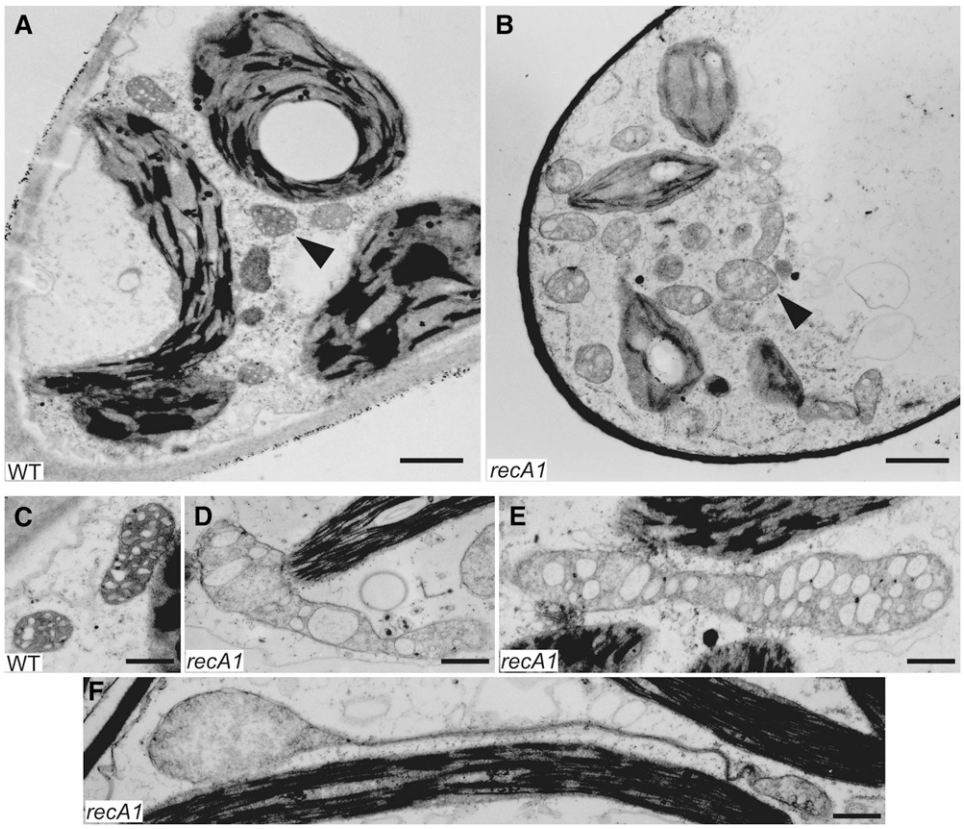

Figure 2. Ultrastructure of Mitochondria in the Protonemal Cell.

Transmission electron micrographs of protonemal cells of the wild-type background (**[A]** and **[C]**) and in *RECA1* insertional disruptants [*recA1(ins)-1*] (**[B]** and **[D]** to **[F]**). The arrowheads indicate mitochondria. Bars = 1 μm in **(A)** and **(B)** and 500 nm in **(C)** to **(F)**.

described above might be caused by aberrant activity of the putative truncated RECA1 protein. To eliminate this possibility, we analyzed a *RECA1* null disruptant in which the complete coding sequence of *RECA1* was removed and replaced with a hygromycin phosphotransferase gene cassette (Odahara et al., 2007). The null disruptant showed phenotypes very similar to those of the insertional disruptant described above (Figures 1D and 1E), in terms of defects in growth and development as well as morphological abnormality of the protonema (Figure 4A). The *nad2-atp9* recombinants accumulated in the null disruptant (Figure 4B) as well as in the insertional disruptant (Figure 3A). For further confirmation, the *RECA1* cDNA was introduced into the nuclear genome of the null disruptant and expressed constitutively. The resulting *RECA1* overexpressor grew normally (Figure 4A), and the signal specific to the *nad2-atp9* recombinant almost disappeared in this strain (Figure 4B). We therefore conclude that the phenotypes of the *RECA1* disruptant, including mtDNA rearrangement, were due to the absence of a functional *RECA1* gene.

Frequent and Multiple Rearrangements of *RECA1* Disruptant mtDNA

The *nad2-atp9* recombinant DNA that accumulated in *RECA1* disruptant mitochondria was a result of aberrant recombination between 69-bp repeats sharing <100% sequence identity. To determine whether other short repeats participate in rearrangements of *RECA1* disruptant mtDNA, we searched for repeats in the *P. patens* mtDNA sequence (Terasawa et al., 2007) using REPuter, a program that identifies repeated sequences (Kurtz and Schleiermacher, 1999). We identified 96 pairs of repeats longer than 40 bp. Among these, the longest is 90 bp, and Table 1 lists 20 sequences with E-values smaller than 5.00×10^{-11}, which includes the *nad2-atp9* repeats (see R10 in Table 1). Intriguingly, many of these repeats (~60%) are located in introns and are oriented as direct repeats (Table 1).

We then focused on three copies of repeats located in the *nad5*, *nad7*, and *nad9* genes (78 to 84 bp long, 96 to 100% identity; R1, R2, and R3 in Table 1; Figure 5A), all of which are oriented as direct repeats, and analyzed the accumulation of DNA molecules resulting from recombination among them. As shown in Figure 5B, through gel blot analysis using *Sac*II-digested genomic DNA and probes hybridizing to the *nad5*, *nad7*, and *nad9* loci, we identified four novel DNA fragments (12.6, 11.1, 3.2, and 1.2 kb) that specifically accumulated in *RECA1* null disruptants. We conclude that these novel *RECA1* disruptant-specific DNA fragments are bona fide DNAs that arose from recombination between the repeats because (1) the sizes of these fragments were consistent with the predicted sizes

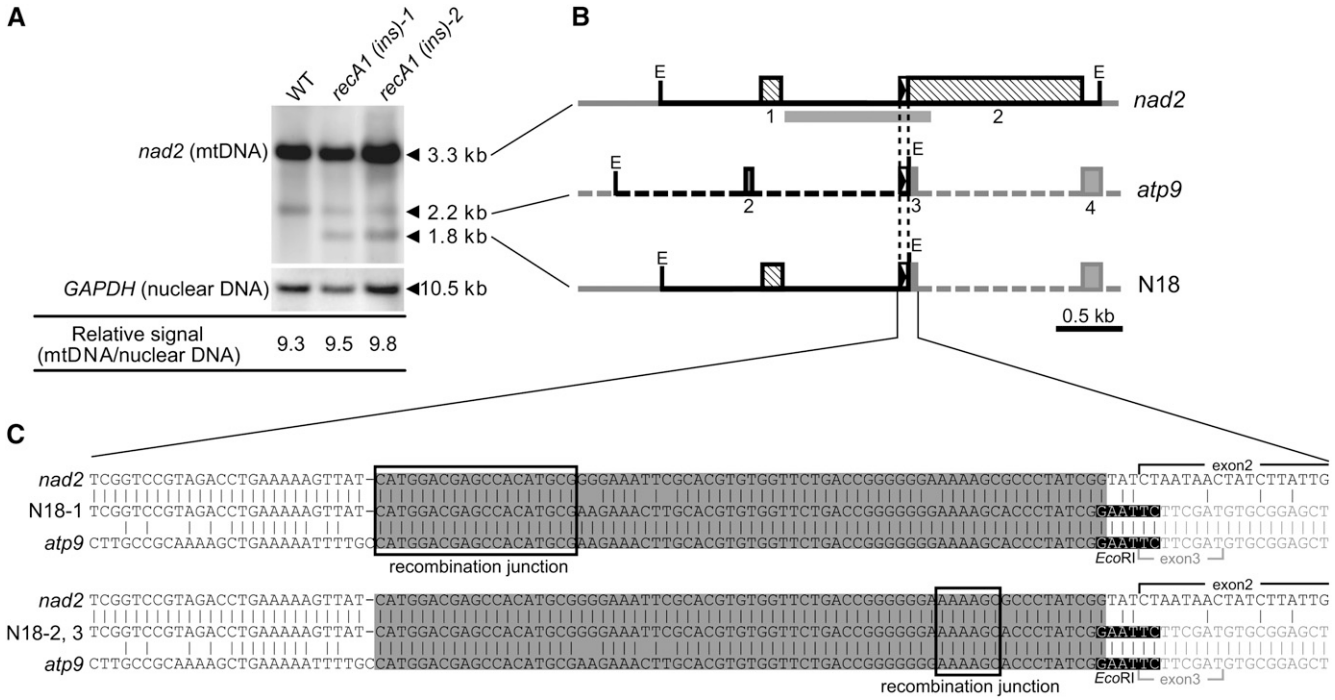

Figure 3. Recombination of mtDNA in *RECA1* Disruptants.

(A) DNA gel blots of total DNA from wild-type cells and *RECA1* disruptants hybridized with the *nad2* and *GAPDH* probes. Total DNA was digested with *Eco*RI. The intensity of *nad2* bands (3.3 kb) relative to that of *GAPDH* on the blot is calculated and shown below the blots.
(B) The structures of *nad2*-related *Eco*RI DNA fragments that were revealed by cloning and DNA sequencing. The *Eco*RI fragments corresponding to the bands on the blot in **(A)** are represented by black lines, and flanking fragments are represented by gray lines. The position of the *nad2* probe used in **(A)** is indicated by a thick gray line. The sequences corresponding to the *nad2* and *atp9* loci are shown by solid and broken lines, respectively. The *Eco*RI recognition sites are indicated by E. The boxes represent exons, and the lines between boxes represent introns and noncoding flanking sequences. Annotated numbers of the exons are shown under the boxes. The repeats (69 bp long, 91% identity) are indicated by the triangles in boxes.
(C) Nucleotide sequences of a region around the recombination junction in three independently obtained clones (N18-1 to -3), compared with those of the corresponding *nad2* and *atp9* loci. The 69-bp repeat sequences are shaded, and recombination is considered to occur within the boxed sequences.

of DNA fragments created by recombination between the repeats (Figures 5A and 5B), even when the genomic DNA was digested with other restriction enzymes (e.g., *Dra*I and *Eco*RI; see Supplemental Figure 1 online), and (2) these novel DNA fragments hybridized to probes used to detect both repeat loci (e.g., a 1.2-kb *Sac*II fragment, which was assumed to be a *nad7-nad9* recombinant, hybridized to both the *nad7* and *nad9* probes; Figure 5B). Accumulation of the predicted recombinants in *RECA1* disruptants was also confirmed by PCR using primers that specifically amplify recombinants and by DNA sequencing of the PCR products. All possible recombinants involving the three copies of the repeats, except for the *nad7-nad5* recombinant and the *nad9-nad5* recombinant, were detectable in this blot (Figure 5B); an explanation for the absence of signals for the two recombinants is provided below (see Discussion). A notable finding in this blot is that the amount of the *nad7-nad9* recombinant in the *recA1-1* strain (1.2 kb, lane 5 in Figure 5B) was equivalent to as much as 40% of the amount of the *nad9* segment in the wild-type background (1.7 kb, lane 4 in Figure 5B), and the amount of the *nad9* segment was correspondingly decreased in the *recA1-1* strain (1.7 kb, lane 5 in Figure 5B), suggesting that ~40% of the *nad9* locus was converted to the *nad7-nad9* recombinant as a consequence of recombination between the 79-bp repeats in the *nad7* and *nad9* genes. By contrast, the amount of the *nad7* segment in the *recA1-1* strain (2.7 kb, lane 2 in Figure 5B) was almost the same as that in the wild-type background (2.7 kb, lane 1 in Figure 5B) in spite of the conversion of a significant amount of the *nad7* segment in the *nad7-nad9* recombinant (1.2 kb, lane 2 in Figure 5B). This means that the *nad7* locus was amplified in the *recA1-1* strain. These results show that frequent and multiple rearrangements, which were likely to be caused by aberrant recombination among the dispersed repeats, occurred in the *RECA1* disruptant mtDNA, resulting in gene truncation and amplification.

Repeated Sequence-Mediated Deletion in *RECA1* Disruptant mtDNA

Recombination between direct repeats in mtDNA can occur intermolecularly or intramolecularly. However, it is difficult to determine how the recombined DNA regions abnormally accumulating in the *RECA1* disruptants were generated, since the DNA was fragmented by digestion with restriction enzymes. The distance between the repeats in the *nad9* and *nad7* loci, in which

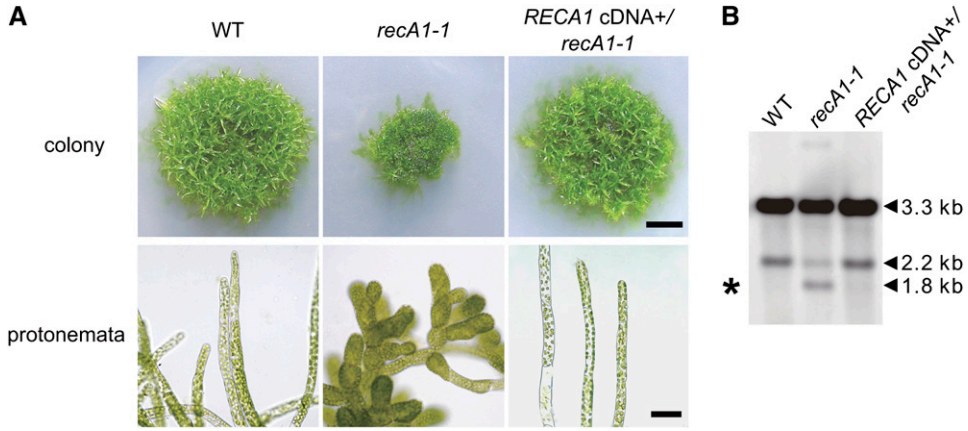

Figure 4. Phenotypes of the *RECA1* Null Disruptant and the *RECA1* cDNA Overexpressor in the *RECA1* Null Background.

(A) Growth and morphology of colonies and protonemata of the wild-type background, the *RECA1* null disruptant (*recA1-1*), and the *RECA1* cDNA overexpressor in the *RECA1* null background (*RECA1* cDNA$^+$/ *recA1-1*). Colonies were cultivated on agar plates for 4 weeks. Bars = 5 mm in top panels and 50 μm in bottom panels.

(B) DNA gel blot analysis of the mtDNA configuration at the *nad2* locus using the *nad2* probe. Total genomic DNA was digested with *Eco*RI. The asterisk indicates the DNA fragment corresponding to *nad2-atp9* recombinant DNA molecules.

[See online article for color version of this figure.]

efficient recombination occurred in the disruptant as shown in Figures 5A and 5B, is 11 kb. To obtain evidence for intramolecular recombination between the *nad9* and *nad7* loci, we examined the generation of an 11-kb circular DNA molecule, which is an expected product of intramolecular recombination (Figure 5C).

DNA gel blot analysis was performed with total DNA extracted from protonema of wild-type and *recA1-1* strains by the cetyltrimethylammonium bromide (CTAB) method, a routine method for extraction of total genomic DNA, and a probe that hybridizes to a region between *nad9* and *nad7*. We detected a specific signal indicative of the predicted 11-kb covalently closed circular DNA in the *RECA1* disruptant (Figure 5D). A more intense signal was detected for DNA prepared from the disruptant by the alkaline lysis method (see Supplemental Figure 2 online), an efficient extraction method for circular plasmids in *E. coli* (Sambrook et al., 1989), suggesting that the DNA has a closed circular structure. Furthermore, another signal was detected for *RECA1* disruptant DNA prepared by the CTAB method (Figure 5D), as well as for that prepared by the alkaline lysis method (see Supplemental Figure 2 online); this might correspond to an undefined subgenome derived from intramolecular recombination between direct repeats other than the *nad9-nad7* repeats and which contains a sequence recognized by the probe. These results demonstrate that intramolecular recombination between direct repeats occurred, and thereby subgenomic molecules with a deletion of part of the mitochondrial genome were indeed generated in *RECA1* disruptant cells.

Recombination between Inverted Repeats

As all the repeats examined above were direct repeats, we tested whether inverted repeats are also involved in rearrangements. By DNA gel blot analysis, we first tried to detect a DNA fragment resulting from recombination between the inverted R15 repeats (62 bp long, 90% identity; Table 1), which are located in intergenic regions. However, there was no apparent accumulation of the DNA fragment in the *RECA1* disruptants as well as in wild-type plants. We then developed a real-time PCR method with primers that specifically amplify the DNA resulting from recombination between the inverted repeats (Figure 6A) and thereby quantified the relative copy number of the recombined DNA in the wild-type background and in *RECA1* disruptants. In *RECA1* disruptants, the calculated relative copy number of the recombined DNA per that of nuclear DNA was found to be 100- to 700-fold higher than in the wild-type background (Figure 6B). This result indicates that aberrant recombination was significantly induced between inverted repeats as well as between direct repeats in *RECA1* disruptant mitochondria and hence demonstrates that repeat orientation is not a prerequisite for the aberrant recombination. With the elevated recombination frequency in the *RECA1* disruptants, the recombined DNA was still not detectable by DNA gel blot analysis as described above, probably because of a relatively low intrinsic tendency of recombination between R15 repeats whose E-value is larger than those of R1-R3 and R10 (see Table 1).

DISCUSSION

Here, we showed that disruption of a *P. patens* mitochondrial *recA* gene (*RECA1*) caused a serious defect in plant growth and development as well as a morphological abnormality in mitochondria. Further analyses of the disruptants revealed frequent and dynamic rearrangements involving multiple loci of the disruptant mtDNA (Figures 3 and 5). The rearrangements were caused by recombination among short (<100 bp) dispersed

Table 1. Repeated Sequences in the *P. patens* Mitochondrial Genome (E-Values <5.00 × 10^{-11}, >40 bp)

	Repeat-1			Repeat-2					
No.	Length (bp)	Position[a]	Locus[b]	Length (bp)	Position	Locus	Orientation[c]	Distance (bp)[d]	E-value[e]
R1	79	79449	*nad9* intron	79	90131	*nad7* 2nd intron	DR	0	8.54E-39
R2	78	43155	*nad5* 1st intron	78	79453	*nad9* intron	DR	1	3.17E-35
R3	83	43147	*nad5* 1st intron	84	90126	*nad7* 2nd intron	DR	3	7.00E-34
R4	90	49768	*nad4* intron	88	73530	*nad1* 2nd intron	DR	6	3.48E-31
R5	57	43453	*nad5* 1st intron	57	70207	*coxIII* intron	DR	1	1.02E-22
R6	56	50033	*nad4* intron	56	73795	*nad1* 2nd intron	DR	1	4.01E-22
R7	73	40892	tRNA-Leu (CAA)	73	40973	tRNA-Leu (TAA)	DR	6	1.64E-21
R8	50	50374	*nad4* intron	50	74200	*nad1* 2nd intron	DR	0	2.46E-21
R9	47	20077	*ccmF* intron	47	102359	*atp9* 1st intron	DR	0	1.58E-19
R10	69	52599	*nad2* intron	69	103603	*atp9* 2nd intron	DR	6	2.95E-19
R11	51	70213	*coxIII* intron	51	80506	*nad9* intron	DR	1	3.74E-19
R12	48	944	–	48	9303	*coxI* 1st intron	DR	1	2.25E-17
R13	51	43459	*nad5* 1st intron	51	80506	*nad9* intron	DR	2	9.04E-17
R14	58	80499	*nad9* intron	58	90545	*nad7* 2nd intron	DR	4	9.81E-17
R15	62	1640	–	62	41363	–	IR	6	2.48E-15
R16	62	43448	*nad5* 1st intron	62	90541	*nad7* 2nd intron	DR	6	2.48E-15
R17	49	58275	*atp6* intron	50	104767	*atp9* 3rd intron	IR	3	4.25E-14
R18	53	70213	*coxIII* intron	53	90552	*nad7* 2nd intron	DR	5	4.59E-12
R19	46	27033	*nad4L* intron	46	29552	*sdh3* intron	DR	3	8.42E-12
R20	48	12919	–	47	101024	–	IR	4	4.72E-11

[a]Smallest number of the position of the repeated sequences corresponding to the *P. patens* mtDNA sequence accession number AB251495 (Terasawa et al., 2007)

[b]Locus of the repeated sequences. –, intergenic region. All the introns listed in this table are group II introns.

[c]DR, direct repeat; IR, inverted repeat.

[d]Differences between Repeat-1 and Repeat-2.

[e]Calculated E-value.

repeated sequences. Our results suggest a role for RECA1 in suppressing recombination among the short repeats that are abundantly scattered throughout the *P. patens* mitochondrial genome.

Our analyses showed that most of the repeats in the *P. patens* mtDNA are located in introns. Recombination between the repeats thus causes truncation (and in some cases, chimerization) of genes, as shown in this article (Figures 3 and 5). The recombination simultaneously generates subgenomes containing the truncated gene. The subgenome exists in some proportion relative to the normal genome, a condition known as heteroplasmy, and when the amount of the normal genome falls below a threshold level required for normal function of mitochondria, a mutant phenotype is seen. The effect of mtDNA heteroplasmy is discussed in a number of studies in maize (*Zea mays*; Gu et al., 1993, 1994; Marienfeld and Newton, 1994). The phenotypes of the *RECA1* disruptant, including the defect in plant growth and development as well as mitochondrial abnormalities, may be caused by the effect of mtDNA heteroplasmy involving the subgenomes with the truncated gene, which were derived from the induced aberrant recombination. In addition, we demonstrated that intramolecular recombination between direct repeats occurred, resulting in the generation of two subgenomic mtDNA molecules, one of which is shown in Figure 5D. If one subgenome becomes predominant over the parental normal genome, the dose of genes existing in another subgenome will decrease. When the gene dosage falls below the threshold level required for normal function of mitochondria, the phenotypic defect of the *RECA1* disruptant could be seen. The apparent absence of a signal corresponding to one of the two reciprocal molecules resulting from recombination between the *nad7* and *nad5* loci as well as between the *nad9* and *nad5* loci (Figure 5B) might be due to the difference in stability between the molecules. This could result in a decrease in the dose of genes existing in the unstable molecule. Such a decrease in the gene dosage might affect the phenotypes of the *RECA1* disruptant; however, it was reported that plant mitochondria are likely to tolerate some extent of variation in gene dosages (Allen et al., 2007).

What is the molecular basis for the suppression of mtDNA rearrangements by RECA1? Functional similarity between RECA1 and *E. coli* RecA is expected from their protein sequence similarity (Odahara et al., 2007). Indeed, plant mitochondrial *recA* genes, including *RECA1*, can partially complement the *E. coli recA* mutation (Khazi et al., 2003; Odahara et al., 2007), and strand transfer activity that is probably related to RecA has been detected in partially purified plant mitochondrial fractions (Manchekar et al., 2006). In an early model of recombinational DNA repair in *E. coli*, RecA binds to single-stranded DNA resulting from the processing of double-strand DNA ends and then promotes strand exchange between homologous sequences to make D-loops (Kowalczykowski et al., 1994). Later studies suggested that RecA and other recombination proteins function

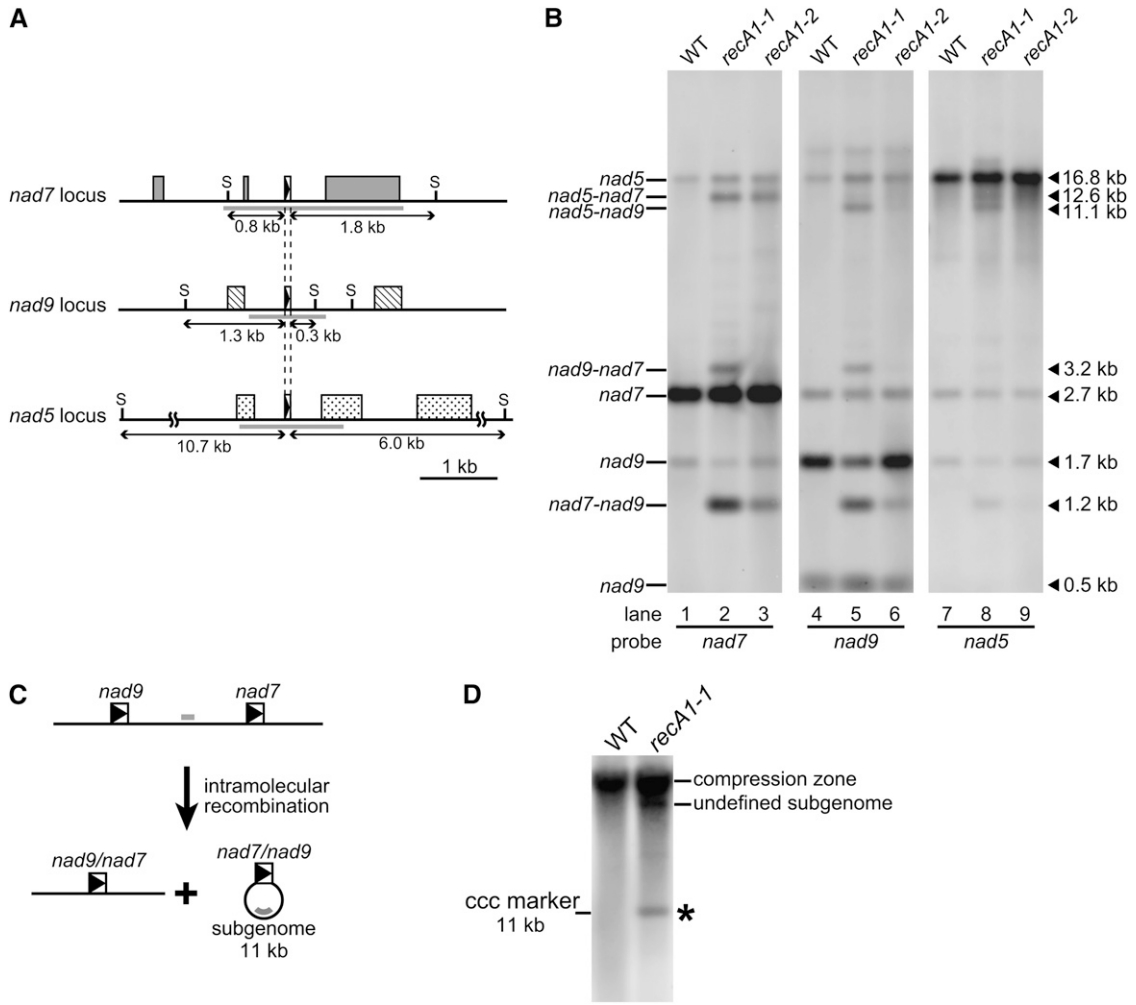

Figure 5. Frequent and Multiple Rearrangements and Repeat-Mediated Deletion of mtDNA.

(A) Schematic representation of the structures of the three copies of repeats located at the *nad7*, *nad9*, and *nad5* loci and the flanking region. The repeats (78 to 84 bp, 96 to 100% identity) are indicated by the triangles in the boxes. The probes used in **(B)** and the *Sac*II recognition sites are indicated by bold gray lines and S, respectively.

(B) Analysis of the mtDNA configuration at the *nad7*, *nad9*, and *nad5* loci. Hybridizations using the probes indicated below the blots were performed with *Sac*II-digested total genomic DNA of the wild-type background and of two *RECA1* null disruptants (*recA1-1* and *recA1-2*). The presumed structures and the lengths of the major bands are indicated on the left and right, respectively.

(C) Scheme for the production of deleted mtDNA by intramolecular recombination between direct repeats. R1 direct repeats shown by the triangles in the boxes are located in both the *nad7* and *nad9* loci, and intramolecular recombination between them generates an 11-kb circular DNA molecule. The probe used in **(D)** is shown by a thick gray line.

(D) Detection of subgenomic molecules by DNA gel blot analysis. Hybridization using the probe designed to detect the genomic region between *nad9* and *nad7* was performed with total genomic DNA of the wild-type background and the *RECA1* null disruptant (*recA1-1*) extracted by the CTAB method. The asterisk indicates subgenomic molecules that comigrated with an 11-kb covalently closed circular (ccc) plasmid.

in the repair of collapsed or stalled replication forks, which are caused by lesions on the template DNA (Cox et al., 2000; Lusetti and Cox, 2002). A collapsed replication fork may be repaired via a D-loop formed by RecA according to the conventional early model of recombinational DNA repair, whereas in the context of repair of a stalled replication fork, RecA is, in some situations, proposed to participate in regression of the fork (Seigneur et al., 2000; Robu et al., 2001) and/or maintenance of the regressed fork (Courcelle and Hanawalt, 2003). Based on models proposed for *E. coli*, a possible explanation for the suppression of DNA rearrangements by RECA1 is illustrated in Figure 7. A collapsed replication fork may be repaired via a D-loop formed by RECA1 to restart replication (Figure 7A). In the absence of RECA1, the DNA end could recombine with a short similar sequence in an ectopic locus by the action of an uncharacterized recombination system that is independent of *RECA1* (Figure 7A). On the other hand, a

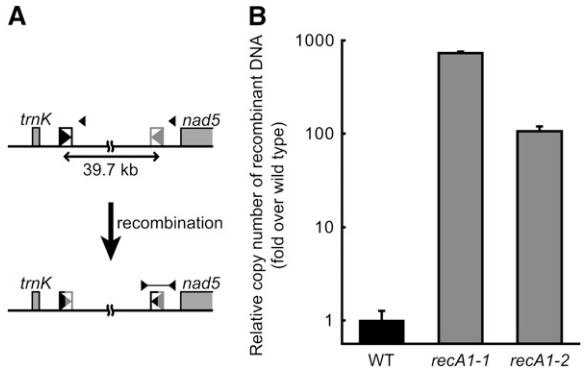

Figure 6. Effect of the *RECA1* Disruption on the Rate of Recombination between Inverted Repeats in mtDNA.

(A) Schematic representation of recombination between R15 inverted repeats. The repeats (62 bp, 90% identity) and flanking genes are indicated by triangles in boxes and gray boxes, respectively. A DNA segment containing the recombination junction can be amplified by PCR using specific primers (shown by arrowheads connected by horizontal line).

(B) Relative copy number of the recombined DNA per nuclear DNA, measured by quantitative real-time PCR. Recombinant DNA in the wild-type background was given a value of 1. Data from three independent PCR reactions are expressed as mean ± SE (n = 3).

stalled replication fork may be processed by the action of RECA1 via regression of the fork (Figure 7B). Without RECA1, an unrepaired stalled replication fork may lead to a rearrangement that involves short repeats (Figure 7B) because stalled forks have been suggested to be a significant cause of ectopic DNA rearrangements mediated by template-switching during replication in bacteria (Slack et al., 2006) and human cells (Lee et al., 2007). The lower rate of mtDNA repair in the *RECA1* disruptant following MMS treatment (Odahara et al., 2007) supports a role for RECA1 in the repair of collapsed or stalled replication forks in mitochondria because replication at MMS-damaged DNA and at single-strand nicks introduced by AP-endonuclease in base excision repair of MMS-damaged bases are suggested to cause stalling and collapse of replication forks, respectively, and RecA-dependent homologous recombination is thought to be essential for fork repair (Nowosielska et al., 2006).

Several *Arabidopsis* nuclear mutations influence the amount of specific DNA molecules generated by recombination between relatively short repeats in mitochondria. Mutation of MutS homolog 1 (*MSH1*), which encodes a homolog of *E. coli* MutS targeted to mitochondria, confers an accumulation of two kinds of mitochondrial DNA: one product is generated by aberrant recombination between two 249-bp repeats; another is generated by recombination between two 335-bp repeats (Abdelnoor et al., 2003; Shedge et al., 2007). A similar accumulation of recombined mitochondrial DNA molecules has been observed in an Organellar Single-stranded DNA Binding protein 1 (*OSB1*) mutant of *Arabidopsis* (Zaegel et al., 2006). In this mutant, four pairs of repeats were reported to be involved in the recombination event: a pair of 435-bp repeats and a pair of 556-bp repeats as well as the two repeat pairs that were studied in the *MSH1* mutant described above. Recently, mutation of *RECA3*, one of three nuclear *recA* homologs in *Arabidopsis*, was reported to induce recombination between the 249-bp repeats in mitochondria (Shedge et al., 2007). Any pair of repeats involved in rearrangements in these *Arabidopsis* mutants is >200 bp and exactly identical, whereas the repeats involved in rearrangements in *RECA1* disruptants are <100 bp and contain some mismatches. Furthermore, the few hot spots for the recombination observed in the *MSH1* and *RECA3* mutants suggests a role for MSH1 and RECA3 in suppression of specific recombination events, whereas the multiple hot spots for recombination in *RECA1* disruptant mtDNA suggest a role for RECA1 in suppression of a broad variety of recombination. These differences in repeats between *Arabidopsis* and *P. patens* may imply that the features of recombination induced in the *RECA1* disruptant are distinct from those in the *Arabidopsis* mutants.

Arabidopsis has two mitochondrial RecA homologs, RECA2 (which also localizes to chloroplasts) and RECA3. It was reported that disruption of *RECA3* results in viable and phenotypically

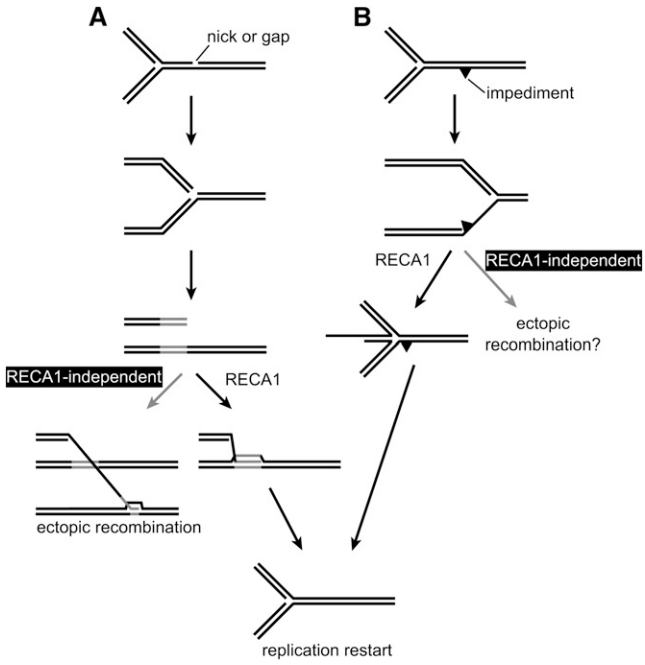

Figure 7. A Model for the Repression of DNA Rearrangements by RECA1 in the Repair of a Collapsed or Stalled Replication Fork.

(A) Repair of a collapsed replication fork by RECA1. A collapsed replication fork can result from the DNA polymerase encountering a nick or a gap on the template DNA. RECA1 may be loaded onto the DNA, and a D-loop is formed between the DNA end and a sister chromosome to restart replication. In the absence of RECA1, the DNA end could initiate recombination independent of RECA1 with a similar short sequence at an ectopic locus.

(B) Repair of a stalled replication fork by RECA1. A replication fork can be stalled by an impediment on the template DNA. RECA1 may promote regression of the stalled fork and/or maintain the regressed fork. After removing the impediment, replication can be restarted. In the absence of RECA1, the presence of the stalled fork leads to ectopic recombination.

normal plants but induces aberrant recombination in the mitochondrial genome, whereas disruption of *RECA2* results in lethality (Shedge et al., 2007). RECA3 uniquely has a truncation in the C-terminal end important for strand exchange and substitutions in conserved amino acids important for ATP binding/hydrolyzing and monomer–monomer interaction (Shedge et al., 2007). The existence of two mitochondrial RecA proteins is reminiscent of functional diversification. Shedge et al. (2007) suggested a role for RECA3 in maintaining mitochondrial genome stability; however, the functional relationship between the two RecA proteins and the contribution of RECA2 to recombination in the mitochondrial genome remain unclear. Our subcellular localization analyses of *P. patens* RecA proteins (Odahara et al., 2007; Inouye et al., 2008) and survey of the *P. patens* nuclear genome sequence (Rensing et al., 2008) show that *P. patens* has a single mitochondrial RecA. Thus, our analyses of *RECA1* clearly show a role for RecA in plant mitochondria, and here we propose that one of the primary roles of plant mitochondrial RecA is to suppress recombination among the short repeats (<100 bp) scattered throughout the genome.

Our analysis of *P. patens* mtDNA showed that most of the 96 pairs of repeats exceeding 40 bp are located in group II introns (Table 1), which are known to be transposable elements (Lambowitz and Zimmerly, 2004). This interesting feature may have arisen by an increase in the number of copies of group II introns by retrotransposition and subsequent base substitutions, except in regions where there are functional constraints on intron splicing, resulting in the conserved short repeats scattered throughout the mtDNA. Therefore, our results suggest that RecA suppresses mitochondrial genome instability caused by this increase in the copy number of repeats, which were amplified via retrotransposition of group II introns. It is possible that genome stabilization by RecA could ensure an increase in the copy number of group II introns.

In this report, we showed abnormally induced rearrangements of the mitochondrial genome in the *RECA1* disruptant. Plant mitochondrial genomes were reported to exhibit a slow rate of nucleotide substitution (Wolfe et al., 1987; Palmer and Herbon, 1988); however, they are occasionally rearranged by recombination between short (<1 kb, in most case <200 bp) repeats (Newton et al., 2004). This suggests that plant mitochondrial genomes can potentially undergo rearrangements. Our results suggest that mtDNA rearrangements might be normally suppressed to a low level by the functioning of a mitochondrial RecA, and when its activity is attenuated, frequent rearrangements might be induced. In the mitochondrial genomes of plants, especially higher plants, short repeats are abundant. RecA-mediated homologous recombination can play a crucial role in suppression of recombination among such dispersed repeats in plant mitochondria, and the role is likely to be indispensable for maintaining mitochondrial genome stability.

METHODS

Plant Material and Growth Conditions

Protonemata of *Physcomitrella patens* Bruch and Schimp subsp *patens* were cultured on cellophane-covered BCDATG agar medium (Nishiyama et al., 2000). Protonemata were cultivated at 25°C under constant light conditions (70 μmol m^{-2} s^{-1}). To compare the growth rate of *RECA1* disruptants with that of wild-type cells, tissues were homogenized using Ultra-Turrax (IKA), and protonemata were subsequently cultivated as described above at least twice, and small pieces (~1.5 mm in diameter) of fresh protonemata were then transferred onto BCDATG agar medium without cellophane and cultivated.

DNA and RNA Extraction

Genomic DNA was extracted by the CTAB method (Murray and Thompson, 1980) from protonemata cultivated for 4 d after inoculation on agar medium.

The alkaline lysis method (Sambrook et al., 1989) was applied for efficient extraction of a species of small circular DNA from protonemata. Protonemata (200 mg) ground in liquid nitrogen were mixed with 400 μL alkaline buffer (0.2 M NaOH and 1% SDS) and incubated on ice for 5 min and then neutralized by adding 300 μL neutralization buffer (3 M potassium acetate and 2 M acetate) and incubated on ice for 5 min. DNA was purified by phenol:chloroform extraction and isopropanol precipitation. For DNA gel blot analysis, 10 ng of the extracted DNA was used.

Total RNA was extracted from protonemata using the RNeasy Plant Mini Kit (Qiagen) according to the manufacturer's protocol and treated with DNaseI to remove contaminating genomic DNA.

Moss Transformation

Isolation of protoplasts and subsequent polyethylene glycol–mediated transformation of *P. patens* were performed according to Nishiyama et al. (2000). To generate stable transformants, 10 μg of linearized targeting construct was introduced, and the resulting transformants were subsequently selected in medium containing 20 μg/mL G418 or 30 μg/mL hygromycin B.

Construction of Vectors for *RECA1* Disruption and *RECA1* cDNA Overexpression

To generate a *RECA1* insertional disruptant, a 1.6-kb fragment spanning the 5′ region and a 1.5-kb fragment spanning the 3′ region of the genomic *RECA1* were amplified by PCR using the following primers (restriction sites are underlined): P1 (5′-CCCTGATCAGGTACCCCCGGGGACATGGCGGGAGCTCTGCGAGTACTTAG-3′) and P2 (5′-CGGGAATTCATCGACACCAGTAGAGCG-3′) for amplification of the 1.6-kb fragment, and P3 (5′-GCGTCTAGATTCACGTGATTGCACAGG-3′) and P4 (5′-CCCAAGCTTCACCATGGGATCCCCTGTCACCTCTAGATTATCAGCATC-3′) for amplification of the 1.5-kb fragment. The resulting 1.6-kb fragment was cleaved with *Kpn*I and *Eco*RI, and the 1.5-kb fragment was cleaved with *Xba*I and ligated to *KpnI*/*Eco*RI- and *Xba*I-cleaved pTN3 (Nishiyama et al., 2000), respectively. The resulting plasmid containing the targeting construct was named pMAK124 and linearized before introduction into *P. patens* protoplasts.

For ectopic expression of *RECA1* cDNA in the *RECA1* null background, plasmid pPpMADS2-7133 carrying a genomic fragment of Pp *MADS2* (Henschel et al., 2002), which is interrupted by a DNA fragment containing the E7133 promoter (Mitsuhara et al., 1996), the *nos* terminator, and the *nptII* gene expression cassette, was used. The coding region of the *RECA1* cDNA was amplified by PCR with cDNA prepared from *P. patens* total RNA and the primers P1 and P5 (5′-GGCGCCCGGGCTACCCTGTCACCTCTAG-3′), digested with *Xma*I, and inserted into the *Xma*I site between the E7133 promoter and the *nos* terminator of pPpMADS2-7133. The resulting plasmid pMAK136 was linearized and then introduced into protoplasts of the *RECA1* null disruptant (Odahara et al., 2007). Two stably transformed strains were obtained, and integration of the

introduced DNA into the genomic DNA and overexpression of *RECA1* cDNA were confirmed by PCR and RT-PCR analysis, respectively, according to Odahara et al. (2007). Since these two strains exhibited very similar phenotypes, only one strain was used for further analyses.

DNA Gel Blot Analysis

Total genomic DNA was separated on a 0.7% agarose gel and blotted onto a nylon membrane. To detect nuclear-encoded *RECA1* (shown in Figure 1) and mitochondrial encoded genes (shown in Figures 4 and 5), 4 and 0.5 μg of total genomic DNA were used, respectively. To prepare probes, PCR was performed using the PCR DIG Probe Synthesis Kit (Roche) and the following primers: P1 and P6 (5′-GTAATACGACTCACTATAGGCAATGTCCTTTTCC-3′) for the *RECA1* probe; P7 (5′-CATGGTGGGATCGGCTAAG-3′) and P8 (5′-TAATACGACTCACTATAGGGGCGAGATAGGAGCATCTGTACC-3′) for the *GAPDH* probe; P9 (5′-GCCTAGGAGGGCGCGTTTGGGAAGACG-3′) and P10 (5′-CCCAGACACATAACTATAGTGCTAGCCG-3′) for the *nad2* probe; P11 (5′-TACTAGGTAGTTGTGTAGCAGGTG-3′) and P12 (5′-ACCCATAATCCCGAGAGCTAATCC-3′) for the *nad5* probe; P13 (5′-CGGGTTAGGGGTACGACAGATAGCG-3′) and P14 (5′-TAATACGACTCACTATAGGGCGAGTAGTTCTATCTATCTACCTCTCC-3′) for the *nad7* probe; P15 (5′-TAGAAGTCTGCAACGAAACGGGCACG-3′) and P16 (5′-CGAAGTGGATTACCTAGTCTCCCAG-3′) for the *nad9* probe; and P17 (5′-TCGTCATACGAGCGGAGCTCGAA-3′) and P18 (5′-CGTAGCCAACAAAGGCTCTGAGAG-3′) for a probe to detect the genomic region between *nad9* and *nad7*. Hybridization of the probes was performed at 39°C, and the membranes were washed in 2× SSC with 0.1% SDS at 25°C and 0.5× SSC with 0.1% SDS at 65°C. Detection of the DIG-labeled probes was performed with Anti-DIG-Alkaline Phosphatase (Roche) and AttoPhos (Promega).

For quantitative estimation of mtDNA and nuclear DNA shown in Figure 3, 4 μg of *Eco*RI-digested total genomic DNA was separated on a 0.7% agarose gel and blotted onto a nylon membrane. The blot was initially hybridized to the DIG-labeled *GAPDH* probe and then washed. The blot was subsequently rehybridized to the DIG-labeled *nad2* probe. The intensities of the signals of *GAPDH* and *nad2* (3.3 kb) on the blot were measured by Typhoon 9210 and ImageQuant (GE Healthcare). The relative copy number of mtDNA per nucleus was calculated by dividing the intensity of the signal of *nad2* by that of *GAPDH*.

RT-PCR Analysis

Reverse transcription was performed using 1 μg of total RNA and an oligo (dT) primer, after which PCR was performed. To amplify a segment of *RECA1*, the primers P19 (5′-GGGAAGCTTCGGGTAGTGGAGATCTTTGG-3′) and P20 (5′-GGTGGTGATACTTTGTTC-3′) were used, and to obtain internal controls, the primers P21 (5′-CATGTTCGAGACGTTCAACGTGCCG-3′) and P22 (5′-GATGGACCAGATTCATCGTACTCGC-3′) were used to amplify a segment of the actin gene. In these experiments, PCR amplification was performed in the exponential amplification phase, and the quantities of amplification products were compared using SYBR Green I (TaKaRa) staining.

Transmission Electron Microscopy

Protonemata of each strain cultivated on agar medium were fixed in 2% glutaraldehyde in 20 mM sodium cacodylate, pH 7.2, and in 2% osmium tetroxide in 20 mM sodium cacodylate, pH 7.2, dehydrated with ethanol, and embedded in Spurr's resin. Thin sections were stained with uranyl acetate and lead citrate and observed with a JEM-1200EX electron microscope (JEOL).

Cloning and Sequencing of the *nad2*-related mtDNA Fragment

*Eco*RI-digested total genomic DNA (4 μg) of the *RECA1* disruptant was separated on a 1.0% agarose gel, and the 3.3-, 2.2-, and 1.8-kb DNA fragments were recovered. Genomic DNA libraries were constructed by cloning these *Eco*RI fragments into the *Mfe*I site of the cloning vector pMSC5 (MoBiTec), and these were introduced into *E. coli* cells by electroporation. Colonies were screened by hybridization (Sambrook et al., 1989) using the DIG-labeled *nad2* probe, and positive clones were selected and sequenced.

Identification of Repeats in *P. patens* Mitochondrial DNA

Repeated sequences in *P. patens* mtDNA (accession number AB251495) were identified with the REPuter program (http://bibiserv.techfak.uni-bielefeld.de/reputer/) with a maximal 6 bp of mismatch permitted. Palindromic sequences were eliminated from the repeats.

PCR Analysis of the DNA Created by Recombination among Repeats in *nad5*, *nad7*, and *nad9*

To analyze the accumulation level of the DNA resulting from recombination among repeats in the *nad5*, *nad7*, and *nad9* locus, PCR was performed using wild-type, *recA1-1*, and *recA1-2* total genomic DNA extracted by the CTAB method and the following primers: P11 and P14 for the *nad5-nad7* recombinant, P13 and P12 for the *nad7-nad5* recombinant, P11 and P16 for the *nad5-nad9* recombinant, P15 and P12 for the *nad9-nad5* recombinant, P13 and P16 for the *nad7-nad9* recombinant, P15 and P14 for the *nad9-nad7* recombinant, and P9 and P10 for the *nad2* locus as an internal control. PCR amplification was performed in the exponential amplification phase. The quantities of amplification products from two independent PCR reactions were compared using agarose gel electrophoresis and ethidium bromide staining. The products were then sequenced, and the recombination junctions were confirmed.

Real-Time PCR Analysis of the DNA Created by Recombination between the R15 Repeats

Real-time PCR was performed with the Applied Biosystems 7500 Fast Real-Time PCR System and POWER SYBR Green Master Mix (Applied Biosystems International) using total genomic DNA extracted by the CTAB method and the primers P23 (5′-CAACCGTCTTCTGTGTCTAGGTC-3′) and P24 (5′-GAAACCGGCCTGCATTACATG-3′) for the 91-bp segment of the nuclear-encoded actin gene, and P25 (5′-TACTAGTCCAATGTCGCCATAAGG-3′) and P26 (5′-ATTCTCGACCACAGGAATTTCC-3′) for the 134-bp segment of the DNA that was generated by recombination between the R15 repeats. The relative copy number of the recombined DNA per nuclear DNA was calculated with SDS software (Applied Biosystems International) using standards consisting of serial dilutions of genomic DNA from the wild-type background to quantify the actin gene and that from *recA1-1* for the recombined DNA.

Accession Number

Sequence data from this article can be found in the GenBank/EMBL database under accession number AB284534 (*RECA1*).

Supplemental Data

The following materials are available in the online version of this article.

Supplemental Figure 1. Multiple Rearrangements of *RECA1* Disruptant mtDNA.

Supplemental Figure 2. Repeat-Mediated Deletion of *RECA1* Disruptant mtDNA.

ACKNOWLEDGMENTS

We thank Tomomichi Fujita and Mitsuyasu Hasebe for technical advice as well as Keiko Umezu and Hisaji Maki for helpful discussion. This work was supported by Japan Society for the Promotion of Science Fellowships (08575 to M.O.), by a Grant-in-Aid for Creative Scientific Research (17GS0314 to Y.S.) from the Japan Society for the Promotion of Science, by the program for the Promotion of Basic Research Activities for Innovative Biosciences (PROBRAIN), and by the Frontier Project "Adaptation and Evolution of Extremophiles."

Received November 29, 2008; revised January 31, 2009; accepted March 23, 2009; published April 7, 2009.

REFERENCES

Abdelnoor, R.V., Yule, R., Elo, A., Christensen, A.C., Meyer-Gauen, G., and Mackenzie, S.A. (2003). Substoichiometric shifting in the plant mitochondrial genome is influenced by a gene homologous to MutS. Proc. Natl. Acad. Sci. USA **100:** 5968–5973.

Allen, J.O., et al. (2007). Comparisons among two fertile and three male-sterile mitochondrial genomes of maize. Genetics **177:** 1173–1192.

Andre, C., Levy, A., and Walbot, V. (1992). Small repeated sequences and the structure of plant mitochondrial genomes. Trends Genet. **8:** 128–132.

Bishop, D.K., Park, D., Xu, L., and Kleckner, N. (1992). DMC1: A meiosis-specific yeast homolog of *E. coli recA* required for recombination, synaptonemal complex formation, and cell cycle progression. Cell **69:** 439–456.

Cao, J., Combs, C., and Jagendorf, A.T. (1997). The chloroplast-located homolog of bacterial DNA recombinase. Plant Cell Physiol. **38:** 1319–1325.

Cerutti, H., and Jagendorf, A.T. (1993). DNA strand-transfer activity in pea (*Pisum sativum* L.) chloroplasts. Plant Physiol. **102:** 145–153.

Cerutti, H., Osman, M., Grandoni, P., and Jagendorf, A.T. (1992). A homolog of *Escherichia coli* RecA protein in plastids of higher plants. Proc. Natl. Acad. Sci. USA **89:** 8068–8072.

Courcelle, J., and Hanawalt, P.C. (2003). RecA-dependent recovery of arrested DNA replication forks. Annu. Rev. Genet. **37:** 611–646.

Cox, M.M., Goodman, M.F., Kreuzer, K.N., Sherratt, D.J., Sandler, S.J., and Marians, K.J. (2000). The importance of repairing stalled replication forks. Nature **404:** 37–41.

Gu, J., Miles, D., and Newton, K.J. (1993). Analysis of leaf sectors in the NCS6 mitochondrial mutant of maize. Plant Cell **5:** 963–971.

Gu, J., Dempsey, S., and Newton, K.J. (1994). Rescue of a maize mitochondrial cytochrome oxidase mutant by tissue culture. Plant J. **6:** 787–794.

Henschel, K., Kofuji, R., Hasebe, M., Saedler, H., Munster, T., and Theissen, G. (2002). Two ancient classes of MIKC-type MADS-box genes are present in the moss *Physcomitrella patens.* Mol. Biol. Evol. **19:** 801–814.

Inouye, T., Odahara, M., Fujita, T., Hasebe, M., and Sekine, Y. (2008). Expression and complementation analyses of a chloroplast-localized homolog of bacterial RecA in the moss *Physcomitrella patens.* Biosci. Biotechnol. Biochem. **72:** 1340–1347.

Jiao, S., Thornsberry, J.M., Elthon, T.E., and Newton, K.J. (2005). Biochemical and molecular characterization of photosystem I deficiency in the NCS6 mitochondrial mutant of maize. Plant Mol. Biol. **57:** 303–313.

Khazi, F.R., Edmondson, A.C., and Nielsen, B.L. (2003). An *Arabidopsis* homologue of bacterial RecA that complements an *E. coli recA* deletion is targeted to plant mitochondria. Mol. Genet. Genomics **269:** 454–463.

Kowalczykowski, S.C., Dixon, D.A., Eggleston, A.K., Lauder, S.D., and Rehrauer, W.M. (1994). Biochemistry of homologous recombination in *Escherichia coli.* Microbiol. Rev. **58:** 401–465.

Kurtz, S., and Schleiermacher, C. (1999). REPuter: Fast computation of maximal repeats in complete genomes. Bioinformatics **15:** 426–427.

Lambowitz, A.M., and Zimmerly, S. (2004). Mobile group II introns. Annu. Rev. Genet. **38:** 1–35.

Lee, J.A., Carvalho, C.M., and Lupski, J.R. (2007). A DNA replication mechanism for generating nonrecurrent rearrangements associated with genomic disorders. Cell **131:** 1235–1247.

Little, J.W., and Mount, D.W. (1982). The SOS regulatory system of *Escherichia coli.* Cell **29:** 11–22.

Lonsdale, D.M., Hodge, T.P., and Fauron, C.M. (1984). The physical map and organisation of the mitochondrial genome from the fertile cytoplasm of maize. Nucleic Acids Res. **12:** 9249–9261.

Lusetti, S.L., and Cox, M.M. (2002). The bacterial RecA protein and the recombinational DNA repair of stalled replication forks. Annu. Rev. Biochem. **71:** 71–100.

Manchekar, M., Scissum-Gunn, K., Song, D., Khazi, F., McLean, S.L., and Nielsen, B.L. (2006). DNA recombination activity in soybean mitochondria. J. Mol. Biol. **356:** 288–299.

Marienfeld, J.R., and Newton, K.J. (1994). The maize NCS2 abnormal growth mutant has a chimeric *nad4-nad7* mitochondrial gene and is associated with reduced complex I function. Genetics **138:** 855–863.

Mitsuhara, I., et al. (1996). Efficient promoter cassettes for enhanced expression of foreign genes in dicotyledonous and monocotyledonous plants. Plant Cell Physiol. **37:** 49–59.

Murray, M.G., and Thompson, W.F. (1980). Rapid isolation of high molecular weight plant DNA. Nucleic Acids Res. **8:** 4321–4325.

Newton, K.J., Gabay-Laughnan, S., and Paepe, R.D. (2004). Mitochondrial mutation in plants. In Plant Mitochondria, D.A. Day, A.H. Millar, and J. Whelan, eds (Dordrecht, The Netherlands: Kluwer Academic Publishers), pp. 121–141.

Nishiyama, T., Hiwatashi, Y., Sakakibara, I., Kato, M., and Hasebe, M. (2000). Tagged mutagenesis and gene-trap in the moss, *Physcomitrella patens* by shuttle mutagenesis. DNA Res. **7:** 9–17.

Nowosielska, A., Smith, S.A., Engelward, B.P., and Marinus, M.G. (2006). Homologous recombination prevents methylation-induced toxicity in *Escherichia coli.* Nucleic Acids Res. **34:** 2258–2268.

Oda, K., Yamato, K., Ohta, E., Nakamura, Y., Takemura, M., Nozato, N., Akashi, K., Kanegae, T., Ogura, Y., Kohchi, T., and Ohyama, K. (1992). Gene organization deduced from the complete sequence of liverwort *Marchantia polymorpha* mitochondrial DNA. A primitive form of plant mitochondrial genome. J. Mol. Biol. **223:** 1–7.

Odahara, M., Inouye, T., Fujita, T., Hasebe, M., and Sekine, Y. (2007). Involvement of mitochondrial-targeted RecA in the repair of mitochondrial DNA in the moss, *Physcomitrella patens.* Genes Genet. Syst. **82:** 43–51.

Palmer, J.D., and Herbon, L.A. (1988). Plant mitochondrial DNA evolves rapidly in structure, but slowly in sequence. J. Mol. Evol. **28:** 87–97.

Pham, P., Bertram, J.G., O'Donnell, M., Woodgate, R., and Goodman, M.F. (2001). A model for SOS-lesion-targeted mutations in *Escherichia coli.* Nature **409:** 366–370.

Rensing, S.A., et al. (2008). The *Physcomitrella* genome reveals evolutionary insights into the conquest of land by plants. Science **319:** 64–69.

Robu, M.E., Inman, R.B., and Cox, M.M. (2001). RecA protein promotes the regression of stalled replication forks *in vitro.* Proc. Natl. Acad. Sci. USA **98:** 8211–8218.

Sambrook, J., Fritsch, E., and Maniatis, T. (1989). Molecular Cloning: A Laboratory Manual. (Cold Spring Harbor, NY: Cold Spring Harbor Laboratory Press).

Schaefer, D.G. (2001). Gene targeting in *Physcomitrella patens.* Curr. Opin. Plant Biol. **4:** 143–150.

Seigneur, M., Ehrlich, S.D., and Michel, B. (2000). RuvABC-dependent double-strand breaks in *dnaBts* mutants require *recA.* Mol. Microbiol. **38:** 565–574.

Shedge, V., Arrieta-Montiel, M., Christensen, A.C., and Mackenzie, S.A. (2007). Plant mitochondrial recombination surveillance requires unusual RecA and MutS homologs. Plant Cell **19:** 1251–1264.

Shinohara, A., Ogawa, H., and Ogawa, T. (1992). Rad51 protein involved in repair and recombination in *S. cerevisiae* is a RecA-like protein. Cell **69:** 457–470.

Slack, A., Thornton, P.C., Magner, D.B., Rosenberg, S.M., and Hastings, P.J. (2006). On the mechanism of gene amplification induced under stress in *Escherichia coli.* PLoS Genet. **2:** e48.

Small, I., Suffolk, R., and Leaver, C.J. (1989). Evolution of plant mitochondrial genomes via substoichiometric intermediates. Cell **58:** 69–76.

Sugiura, C., Kobayashi, Y., Aoki, S., Sugita, C., and Sugita, M. (2003). Complete chloroplast DNA sequence of the moss *Physcomitrella patens*: Evidence for the loss and relocation of *rpoA* from the chloroplast to the nucleus. Nucleic Acids Res. **31:** 5324–5331.

Terasawa, K., Odahara, M., Kabeya, Y., Kikugawa, T., Sekine, Y., Fujiwara, M., and Sato, N. (2007). The mitochondrial genome of the moss *Physcomitrella patens* sheds new light on mitochondrial evolution in land plants. Mol. Biol. Evol. **24:** 699–709.

Unseld, M., Marienfeld, J.R., Brandt, P., and Brennicke, A. (1997). The mitochondrial genome of *Arabidopsis thaliana* contains 57 genes in 366,924 nucleotides. Nat. Genet. **15:** 57–61.

Wolfe, K.H., Li, W.H., and Sharp, P.M. (1987). Rates of nucleotide substitution vary greatly among plant mitochondrial, chloroplast, and nuclear DNAs. Proc. Natl. Acad. Sci. USA **84:** 9054–9058.

Zaegel, V., Guermann, B., Le Ret, M., Andres, C., Meyer, D., Erhardt, M., Canaday, J., Gualberto, J.M., and Imbault, P. (2006). The plant-specific ssDNA binding protein OSB1 is involved in the stoichiometric transmission of mitochondrial DNA in *Arabidopsis.* Plant Cell **18:** 3548–3563.